Article **Journal of Technological Engineering**
June, 2021 Vol.5 No.15 17-35

Direct design process of aerodynamic profiles using the Joukowsky transformation

Proceso de diseño directo de perfiles aerodinámicos mediante la transformación de Joukowsky

ROMERO-GÓMEZ, Gabriel Adrián†* & LÓPEZ-GARZA, Víctor

Universidad Michoacana de San Nicolás de Hidalgo, Facultad de Ingeniería Mecánica. Ciudad Universitaria, Colonia Felicitas del Rio 58060 Morelia, México.

ID 1st Author *Gabriel Adrián, Romero-Gómez* / **ORC ID:** 0000-0001-7841-8472

ID 1st Co-autor: *Víctor, López-Garza* / **ORC ID:** 0000-0001-9090-9119, **Researcher ID Thomson:** H-6969-2018, **Open ID:** 10747067300784159738 2, **CVU CONACYT ID:** 55431

DOI: 10.35429/JTEN.2021.15.5.17.35 Received March 14, 2021; Accepted June 29, 2021

Abstract

This document shows the results of a part of the direct design process of airfoils. The research and design of these geometric shapes are of great relevance for their application in aerodynamic devices, since, if a wing profile with a great aerodynamic fineness is developed, the efficiency of the devices that have this geometric shape will be improved on its wings, propellers, etc. This project started from two analytical processes, the first was to obtain the shape of the wing profiles through the Joukowsky transformation, later the pressure distribution of each aerodynamic profile was obtained through the methodology developed by Theodorsen, the profiles that achieved optimal results were subjected to the third and last analysis in the Qblade software, this software allows to find the angle of attack that produces the maximum aerodynamic fineness, in addition to an approximation to the lift and drag coefficients, in this way several curved and aerodynamic profiles were obtained. Various thicknesses whose aerodynamic fines range between 100 and 250 at the optimum angle of attack.

Aerodynamic Fineness, Direct design process, Joukowsky transformation, Theodorsen methodology

Resumen

Este documento muestra los resultados de una parte del proceso de diseño directo de un perfil alar. La investigación y el diseño de estas formas geométricas son de gran relevancia para su aplicación en dispositivos aerodinámicos, ya que, si se llega a desarrollar un perfil alar con una gran fineza aerodinámica, se mejorará la eficiencia de los dispositivos que cuente con estaforma geométrica en sus alas, hélices, etc. Este proyecto partió de dos procesos analíticos, el primero fue obtener la forma de los perfiles alares a través de la transformación de Joukowsky, posteriormente se obtuvo la distribución de presiones de cada perfil aerodinámico mediante la metodología desarrollada por Theodorsen, algunos de perfiles que consiguieron resultados óptimos fueron sometidos al tercer y último análisis en el software Qblade, este software permite encontrar el ángulo de ataque que produce la máxima fineza aerodinámica, además de una aproximación a los coeficientes de sustentación y arrastre, de esta forma se obtuvieron varios perfiles aerodinámicos curvos y de diversos espesores cuyas finezas aerodinámicas oscilan entre 100 y 250 en el ángulo de ataque óptimo.

Fineza aerodinámica, Proceso de diseño directo, Transformación de Joukowsky, Metodología de Theodorsen

Citation: ROMERO-GÓMEZ, Gabriel Adrián & LÓPEZ-GARZA, Víctor. Direct design process of aerodynamic profiles using the Joukowsky transformation. Journal of Technological Engineering. 2021. 5-15: 17-35

* Correspondence to Author (e-mail: grog160998@gmail.com)
† Researcher contributing as first author.

Introduction

The design process of an aerodynamic profile or aerodynamic profile is usually complex, since these geometries must be applied to the cross-sections of the wings that will perform the task of supporting any aircraft in the air, this in the particular case of aerial vehicles. Aerodynamic profiles intended for subsonic aircraft generally have a great thickness in their geometry necessary to facilitate the generation of the force that sustains said aircraft in the air [2] pp. 92-93, however, due to the thickness of the wing profile, the amount of air hitting the airfoil is greater and consequently the drag force increases.

The drag force is that dynamic effect that opposes the displacement of the aircraft in the sky and this impairs the efficiency of the aerodynamic profile, this means that a profile whose thickness is less will generate less lift and drag compared to another medium or thick thickness, although a different way of increasing the support force without increasing the thickness of the profile is by generating a curvature in the trajectory of the profile contour, so the objective of the design of aerodynamic profiles in the present work was to obtain aerodynamic curves profiles, this To obtain specimens whose aerodynamic fineness is the highest possible, said fineness is the relationship between lift and drag force.

For the design of the aerodynamic profiles, a direct design process was used, which consists in that, based on the geometry of the wing profile, its aerodynamic properties are quantified and according to the results of the analysis it is decided if the profile is suitable for application. The geometries were obtained through an analytical process, this method is the result of a transformation of complex numbers known as conformal transformation, said transformation was carried out by the mechanical engineer Nikolái Yegórovich Joukowsky, for this reason this method was named in his honor as the Joukowsky transformation. The next step, after obtaining the geometries of the wing profiles, through the conformal transformation, was to study the profiles using the methodology developed by Theodorsen, this being the first approximation in our research project to the velocity and pressure distributions of the profiles.

Based on the results obtained, only those profiles whose pressure distributions were convenient for the research objective were selected, after the above, the selected profiles were studied in the Qblade software, thus obtaining profiles with a coefficient relationship of lift with respect to the drag coefficient up to 250. The hypothesis is that the profiles can develop better lift coefficients by introducing in them an adequate curvature in the geometry of the aerodynamic profile.

We will divide the present work into three sections, the first one quickly deals with what the Joukowsky transformation is, as well as showing the graphs of the profiles plotted in the Matlab software; the second section shows the pressure distributions in the aerodynamic profiles resulting from the Theodorsen method; and finally, the third section shows the results obtained in the Qblade software.

1. Profiles obtained by the Joukowsky transformation.

The Joukowsky transformation is a type of complex point-to-point transformation that allows transforming a region of complex numbers to another pre-established by the first and also preserving the angles of the original region, due to the aforementioned properties, this type of transformation is called as conformal transformation. Joukowsky, using the parametric equation of the circumference and a suitable conformal transformation, managed to develop a methodology to achieve wing profile geometries.

According to [3], p. 129, the Joukowsky transformation is defined as follows.

$$Y = f + \frac{C^2}{16f} \tag{1}$$

The variable $"Y"$ symbolizes the complex function that represents the points in the transformed plane that has the shape of the aerodynamic profile, $"f"$ is another complex function that describes the points of the closed curve of the circumference and the constant $"\frac{C^2}{16}"$ is equal to the coordinate on the axis of the real numbers where the transformation is not conforming.

For the complex transformation, in the coordinate of the circumference, to be conformal, this coordinate must comply with the first theorem of the conformal mapping.

"If f (z) is analytical and f´ (z) ≠ 0 in a region R, then the transformation w = f (z) is conformal at all points of R" Spiegel et al., (1991), cited by [5].

To simplify the transformation in the present work, this formula was manipulated to express it mathematically as follows.

$$z' = z + \frac{b^2}{z} \quad (2)$$

The letter "z" corresponds to the complex analytical function of the first region that represents the curve of the circumference, and its equation is the following.

$$z = -b + a\,(e^{i\beta} + e^{it}) \quad (3)$$

The complex variable "z´" is the corresponding curve that describes the wing profile, while "b", "a", "β" and "t" are the point of the trailing edge or the coordinate where the transformation does not it conforms due to the abrupt change in the angle tangent to the curve, the radius of the circumference, the angle of elevation of the circumference, and the variable whose range goes from zero to twice pi. The following figures show the parameters in better detail.

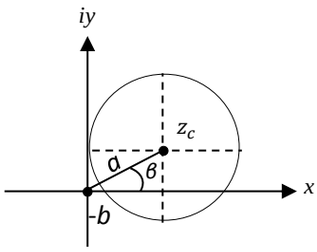

Figure 1.1 Established region of the variable "*z*"

In Figure 1.1 you can see the closed curve that describes the complex analytical function "z", in addition, the parameters "b", "a" and "β" are indicated, which define the position and radius of the circumference, in addition, "z_c" is the coordinate of the center of the circle.

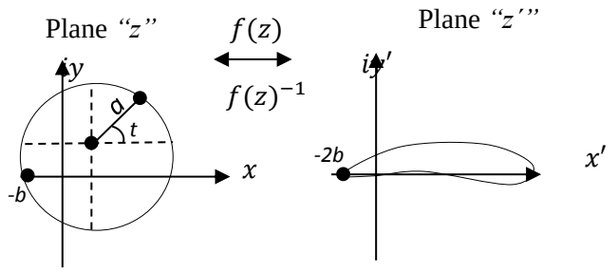

Figure 1.2 "z" and "z´" planes

Figure 1.2 shows the "z" plane and the transformed "z´" plane, the two-way arrow indicates that the process is reversible, that is, from a circumference through the transformation as an aerodynamic profile can be obtained and vice versa. The larger the ratio between "b" and "a", the thinner the profile. It should be noted that this ratio should not exceed one and the greater the magnitude of "β" the profile will have a more pronounced curvature, however, it is recommended that this value does not exceed ten degrees.

From this transformation, the coordinates of the curves of the wing profiles were obtained, whose geometric properties are reflected in the nomenclature that was implemented. First in the nomenclature, it is written in capital letter *"R"* which refers to the relationship between "b" and *"a"* and next to this its value, later it is written, in the same way, in capital letter *"B"* which makes reference to the magnitude in sexagesimal degrees of the beta parameter and, as the last data, *"A"* that indicates the degree of inclination of the profile with respect to the horizontal axis which was plotted, that is, its angle of attack.

Table 1.1 lists the profiles developed through the Joukowsky transformation, in addition to including the maximum thickness in percentage of the chord of the profile, the position of the maximum thickness in percentage of the chord, the maximum curvature and the position of the maximum curvature in percentage of the chord or also called the maximum ordinate. Next, it is shown, from Figure 1.3 to Figure 1.7, the geometries of the aerodynamic profiles listed in Table 1.1.

Aerodynamic profile code	Maximum thickness in percentage of the rope.	Maximum chord thickness position in percent
R0.9B5A0	12.55	24.7
R0.95B5A0	6.02	24.2
R0.85B10A0	18.13	24.4
R0.87B10A0	15.51	23.5
R0.9B10A0	11.35	24.48
R0.92B10A0	8.78	24.49
Aerodynamic profile code	**Maximum curvature**	**Maximum ordinate in percent of the chord.**
R0.9B5A0	4.35	50.5
R0.95B5A0	4.37	48.5
R0.85B10A0	8.24	50.8
R0.87B10A0	8.29	52
R0.9B10A0	8.82	49.28
R0.92B10A0	8.82	50.09

Table 1.1 List of profiles obtained by Joukowsky transformation

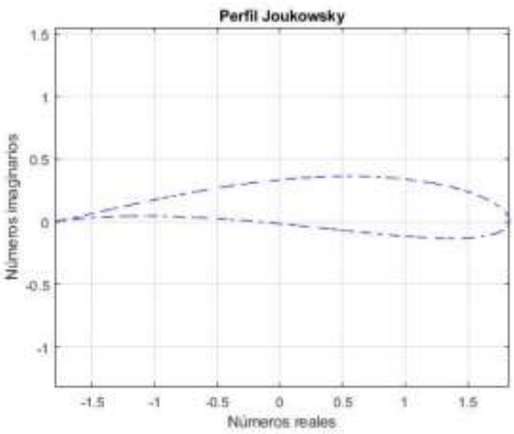

Figure 1.3 Profile R0.9B5A0

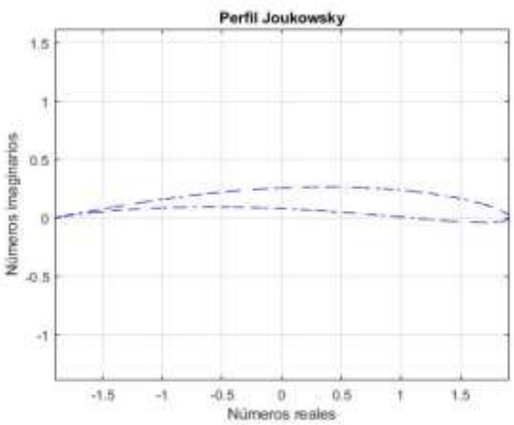

Figure 1.4 Profile R0.95B5A0

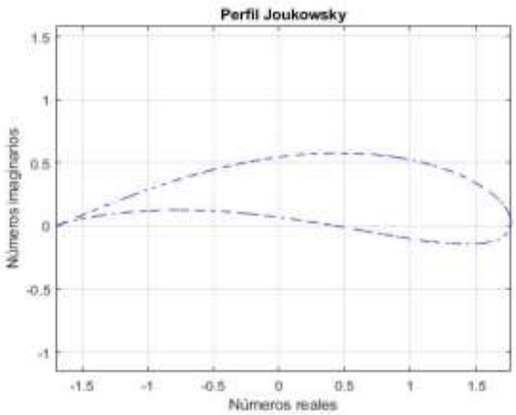

Figure 1.5 Profile R0.85B10A0

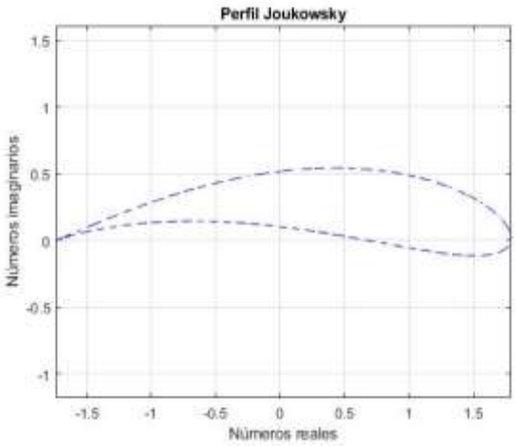

Figure 1.6 Profile R0.87B10A0

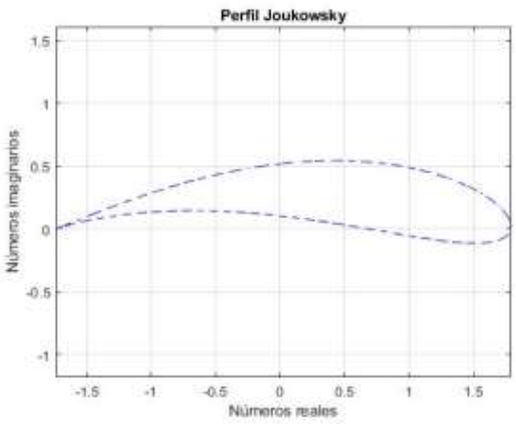

Figure 1.7 Profile R0.9B10A0

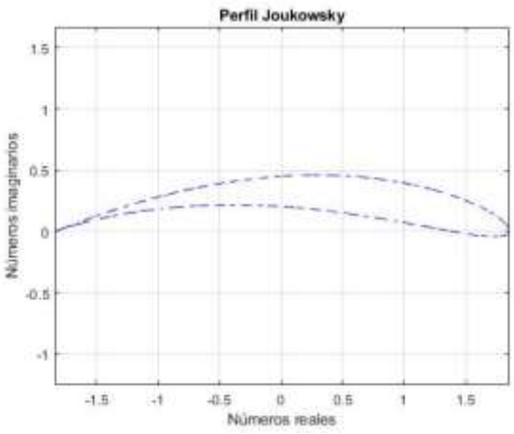

Figure 1.8 Profile R0.92B10A0

2. Theodorsen method

It has been shown that the potential flow field of a cylinder can be related to a potential flow of an airfoil by conformal transformation. Theodorsen implemented, through the relationship, a methodology in an analytical way to obtain the pressure and velocity distribution of the streamlines that circulate around any aerodynamic profile. This methodology was obtained from [5].

The results obtained were for the profiles located in Table 1.1, at an angle of attack identical to zero, this because the aerodynamic fineness tends to increase when the angle of attack increases, therefore, if the profile generates a satisfactory distribution when those airfoils are in a horizontal position, this distribution improves as the angle of attack increases. The result of this methodology is only an approximation to the real effects caused by the flow, since the analysis is carried out under the assumptions of incompressible air, ideal fluid and irrotational flow.

Next, the graphs of the distributions of the pressure coefficient, corresponding to the vertical axis, with respect to the percentage of the chord of each one of the profiles, corresponding to the horizontal axis, are presented; Figure 2.1, Figure 2.2, Figure 2.3, Figure 2.4, Figure 2.5 and Figure 2.6.

The results of the coefficient of pressure around the airfoil were used to calculate the coefficient of lift using the following formula.

$$Cl = \int_{Li}^{Ls} \left[\frac{Cp(x)_{Extrados} - Cp(x)_{Intrados}}{Ls - Li} \right] dx \quad (4)$$

The difference "Ls - Li" represents the chord of the aerodynamic profile and "Cp (x) $Extrados$" the local pressure coefficient in each of the coordinates along the chord of the profile on the extrados as a function of $"x"$, while "Cp (x) $Intrados$" is the local pressure coefficient in the intrados as a function of $"x"$. The integration was applied for each of the profiles. Graph 2.1 shows the lift coefficient of each of the aerodynamic profiles based on equation number four and the results obtained using Theodorsen's method.

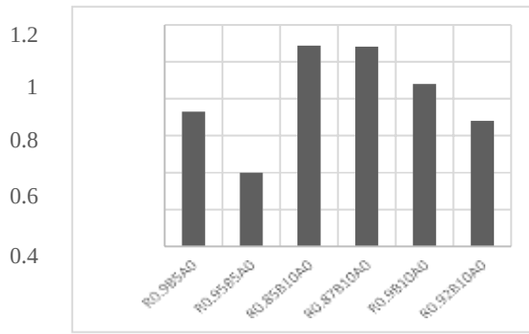

Graph 2.1 Support coefficients of the profiles

In Graph 2.1 the R0.9B5A0 profile was the geometry that generated the lowest lift coefficient of all the aerodynamic profiles. This result was already expected since the pressure distribution of the profile was obtained, which is represented in Figure 2.2, however, its study continued because it is the thinnest profile of the six, and that, due to its little thickness, the drag coefficient was expected to be much less than its lift coefficient. Another equation deduced by William Kutta and Joukowsky was the equation that calculates the circulation generated by an aerodynamic profile, mathematically it is expressed as follows.

$$\Gamma = 4\pi U_{\infty} a Sen(\alpha \pm \beta) \quad (5)$$

Substituting the circulation equation, equation (5), with respect to the Kutta-Joukowsky theorem equation, a mathematical formula is obtained capable of calculating the lift force of a wing profile.

$$L = 4\pi\rho {U_{\infty}}^2 a Sen(\alpha \pm \beta) \quad (6)$$

Therefore, assuming that the surface of the wing profile is equal to twice the radius of the circumference of the foreground, the lift coefficient will be as follows.

$$CL = 2\pi Sen(\alpha \pm \beta) \quad (7)$$

"Γ" is the flow generated by the aerodynamic profile, "U_∞" is the speed of the free stream, "a" is the radius of the circumference, "α" is the angle of attack and "β" is the angle of elevation. of the circumference.

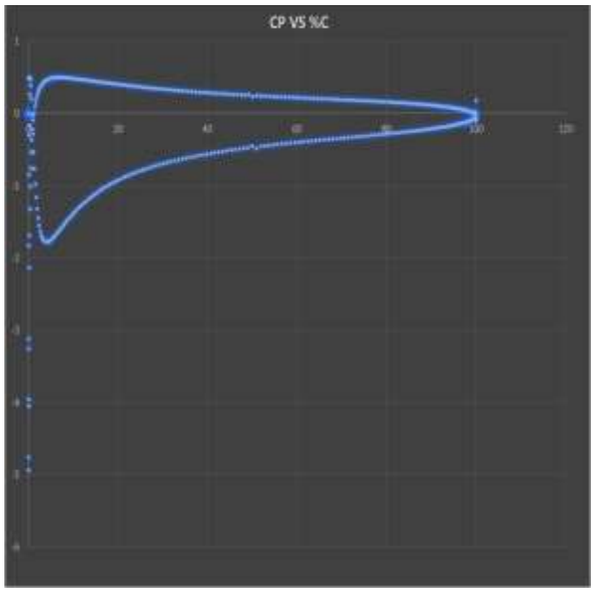

Figure 2.1 Pressure distribution of profile R0.9B5A0

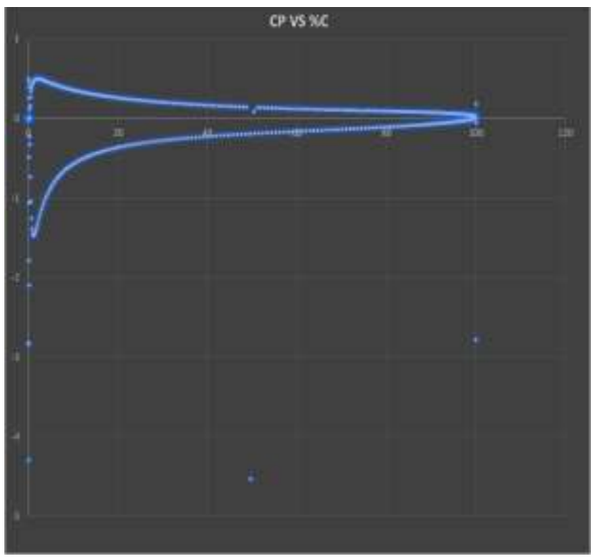

Figure 2.2 Pressure distribution of profile R0.95B5A0

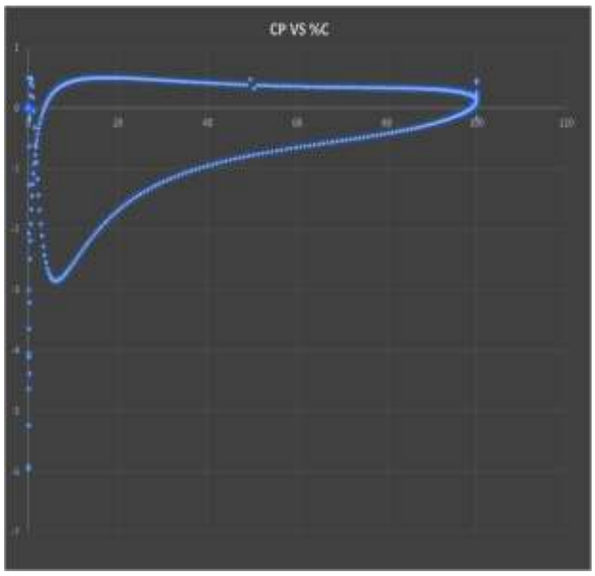

Figure 2.3 Pressure distribution of profile R0.85B10A0

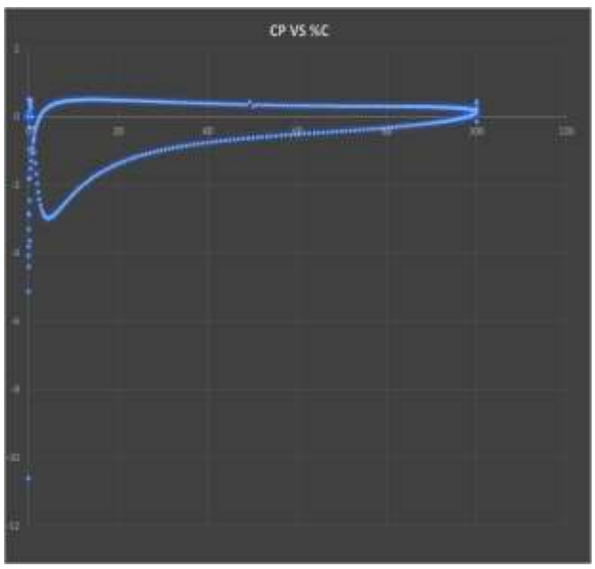

Figure 2.4 Pressure distribution of profile R0.87B10A0

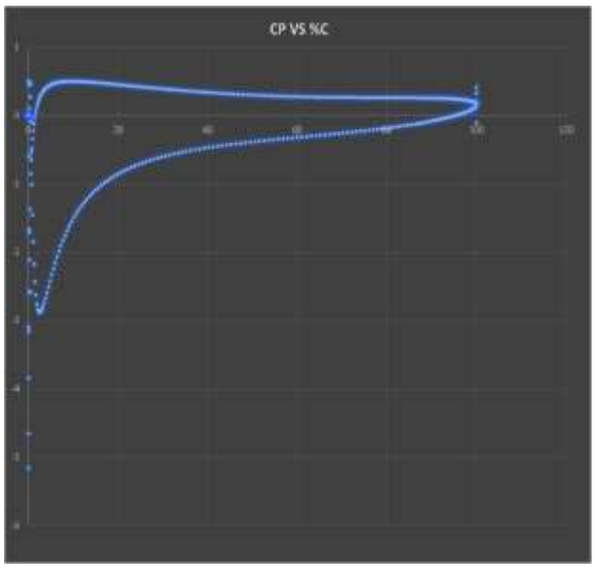

Figure 2.5 Pressure distribution of profile R0.9B10A

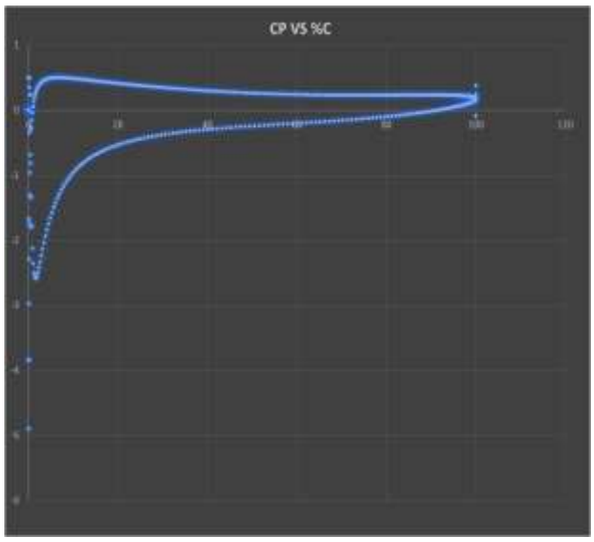

Figure 2.6 Pressure distribution of profile R0.92B10A0

Comparing the results obtained, it was observed that different results are obtained between both methodologies. The aerodynamic profile shown in Figure 1.3, is a profile of medium thickness, the generation of the pressure coefficients is satisfactory, according to the Theodorsen method the lift coefficient "Cl" is 0.73, this value is close to the value of the coefficient lift of 0.54, from equation (7), however, the deviation between the two values is -25% with respect to the Theodorsen method. The approximation has a substantial difference with respect to the method developed by Theodorsen, being, in this case, the different results due to the thickness of the profile.

The aerodynamic profile shown in Figure 1.4, is a thin thickness profile, the generation of the pressure coefficients is satisfactory, according to the Theodorsen method the lift coefficient "Cl" is 0.4, this value is close to the value of the coefficient lift of 0.54, from equation (7), however, the deviation between the two values is 35% with respect to Theodorsen's method. The approximation has a substantial difference with respect to the method developed by Theodorsen, being, in this case, the different results due to the thickness of the profile.

The aerodynamic profile, shown in Figure 1.5, is a thick thickness profile, the generation of the pressure coefficients is satisfactory, according to the Theodorsen method the lift coefficient "Cl" is 1.088, this value is quite close to the value of the lift coefficient of 1.095, from equation (7), the deviation between the two values is 0.28% with respect to the Theodorsen method.

The aerodynamic profile, shown in Figure 1.6, is a medium thickness profile, the generation of the pressure coefficients is satisfactory, according to the Theodorsen method the lift coefficient "Cl" is 1.082, this value is quite close to the value of the lift coefficient of 1.095, from equation (7), the deviation between the two values is 1.2% with respect to the Theodorsen method.

The aerodynamic profile, shown in Figure 1.7, is a profile of medium thickness, the generation of the pressure coefficients is satisfactory, according to the Theodorsen method the lift coefficient "Cl" is 0.88, this value is close to the value of the lift coefficient of 1.095, from equation (7), however, the deviation has an important value between the two values, being 24.43% with respect to the Theodorsen method. The approximation has a substantial difference with respect to the method developed by Theodorsen, being in this case, the thickness of the profile the cause of the difference.

The aerodynamic profile, shown in Figure 1.8, is a profile of thin thickness, the generation of the pressure coefficients is satisfactory, according to the Theodorsen method the lift coefficient "Cl" is 0.68, this value deviates to the value of the lift coefficient of 1.095, from equation (7), however, the deviation between the two values is 61% with respect to the Theodorsen method. The approximation has a substantial difference with respect to the method developed by Theodorsen, being, in this case, the thickness of the profile the cause of the difference.

3. Analysis in Qblade

Qblade is a wind turbine calculation software, the integration of the XFOIL / XFLR5 functionality allows to design custom aerodynamic profiles and calculate their performance poles, this being an excellent tool for the purpose of research.

The results made it possible to obtain the angle of attack that provides the greatest aerodynamic finesse in addition to the drag and lift coefficients. Next, the figures of the graphs are presented, with parameters of the Reynolds number indicated in each of the figures of the order in millions of units.

ISSN 2523-6776

Figure 3.1, Figure 3.2 and Figure 3.3 are the results in the Qblade software of the R0.9B5 profile at different Reynolds numbers of the order of millions and different angles of attack.

Figure 3.1 shows that the highest coefficient of resistance occurs at an angle of attack of twenty degrees, this being around 0.09, however, they are satisfactory results due to their reduced magnitudes.

Figure 3.2 indicates that the lift coefficient falls at an angle of attack around 7.5, because the graphs of the lift coefficient against the angle of attack are no longer linear, the value at this angle of attack is 1.4.

Figure 3.3 shows that the best aerodynamic fineness produced by the profile occurs at an angle of attack of 4 degrees of camber, the corresponding value of the aerodynamic fineness at this angle of attack is around 140 to 155.

Figure 3.4, Figure 3.5 and Figure 3.6 and 3.6 are the results in the Qblade software of the profile R0.95B5 at different Reynolds numbers and angles of attack.

Figure 3.4 shows that the highest drag coefficient occurs at an angle of 20 degrees, the values of this coefficient increase dramatically after an angle of attack of 10 degrees. The magnitudes of the drag coefficients, for angles of attack less than 10 degrees, are less than 0.05, this result is quite satisfactory.

Figure 3.5 indicates that the lift coefficient does not drop to the angle of attack around ten degrees, this being a somewhat satisfactory result. The lift coefficient values range from 1.2 to 1.6.

Figure 3.6 shows that the best aerodynamic fineness produced by the profile is given at an angle of attack of 2.3 degrees of camber, the corresponding value of the aerodynamic fineness at this angle of attack is 130 to 157.

Figure 3.7, Figure 3.8 and Figure 3.9 are the results in the Qblade software of the profile R0.85B10.

Figure 3.7 shows that the highest drag coefficient occurs at an angle of attack around twenty degrees, this being its value between 0.09 and 0.1.

Figure 3.8 indicates that the lift coefficient does not drop at the angle of attack of about twenty degrees, this being a very satisfactory result. The lift coefficient values range from 1.8 to 2. Its graph is linear up to an angle of attack value of 7 degrees.

Figure 3.9 shows that the best aerodynamic fineness produced by the profile is given at an angle of attack of 4 degrees of lean, the corresponding value of the aerodynamic fineness at this angle of attack is 142 to 220.

Figures 3.10, 3.11 and 3.12 are the results in the Qblade software of the profile R0.87B10.

Figure 3.10 shows that the highest drag coefficient occurs at an angle of attack of around twenty degrees, this being its value between 0.8 and 0.12. However, under small angles of attack, the values of the drag coefficient are low.

Figure 3.11 indicates that the lift coefficient does not drop at the angle of attack of about eight degrees, this being a very satisfactory result. The lift coefficient values range from 1.7 to 1.8.

Figure 3.12 shows that the best aerodynamic fineness produced by the profile is given at an angle of attack of 4 degrees of lean, the corresponding value of the aerodynamic fineness at this angle of attack is 159 to 224.

Figure 3.13, Figure 3.14 and Figure 3.15 are the results in the Qblade software of the profile R0.9B10.

Figure 3.13 shows that the highest drag coefficient occurs at an angle of attack of around twenty degrees, this being its value between 0.8 and 0.12. However, the magnitudes of the drag coefficient are reduced for angles of attack less than 10 degrees.

ISSN 2523-6776

Figure 3.14 indicates that the lift coefficient does not drop to the angle of attack of about twenty degrees, this being a very satisfactory result. The lift coefficient values range from 1.5 to 1.9. It must be said that there is a variation in the graph within the line at an angle of attack of four degrees, however, this fact must be verified in a wind tunnel. The coefficient drops to an approximate angle of attack of 7 degrees.

Figure 3.15 shows that the best aerodynamic fineness produced by the profile is given at an angle of attack of 4 degrees lean, the corresponding value of the aerodynamic fineness at this angle of attack is between the range of 175 to 225.

Figure 3.16, Figure 3.17 and Figure 3.18 are the results in the Qblade software of the profile R0.92B10.

Figure 3.16 shows that the highest coefficient of resistance occurs at an angle of attack of around twenty degrees, this being its value between 0.07 and 0.16. For angles of attack less than 10 degrees, the magnitudes of the drag coefficient are less than 0.025, being a satisfactory result.

Figure 3.17 indicates that the lift coefficient does not drop to the angle of attack around eight degrees, this being a very satisfactory result. The lift coefficient values range from 1.6.

Figure 3.18 shows that the best aerodynamic fineness produced by the profile is given at an angle of attack between 4 to 5 degrees of lean, the corresponding value of the aerodynamic fineness at this angle of attack is 200 to 250.

The results in the XFOIL analysis are very close to that of equation number (7), this corroborates that the lift coefficients are close to those that the Kutta-Joukowsky theorem equation quantifies, the Theodorsen method instead is only Accurate for certain profiles of medium thickness and thick profiles.

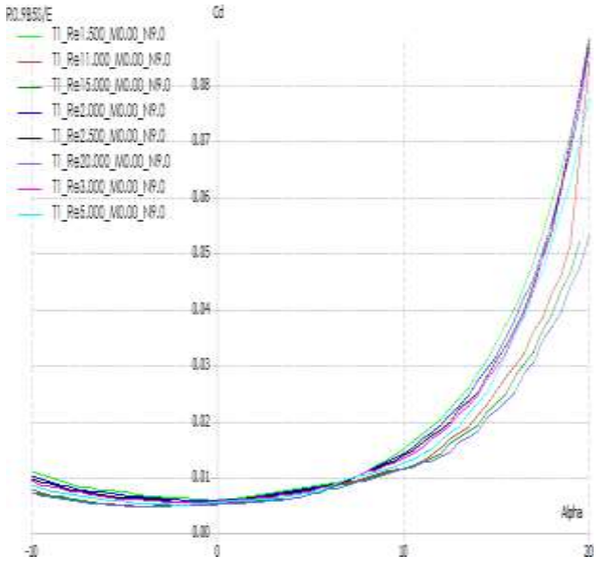

Figure 3.1 Results of the Qblade software of the profile R0.9B5 drag coefficient against the angle of attack.

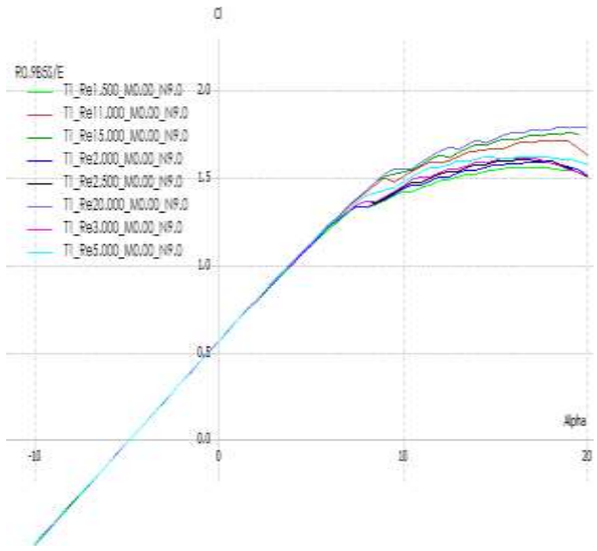

Figure 3.2 Results of the Qblade software of the R0.9B5 profile coefficient of lift versus angle of attack.

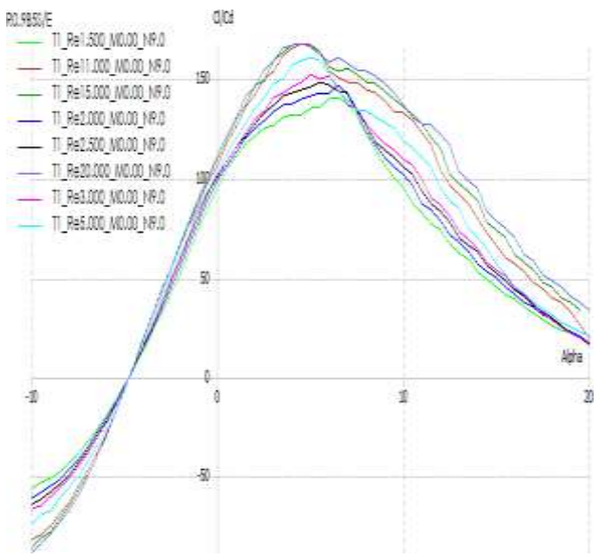

Figure 3.3 Results of the Qblade software of the profile R0.9B5 aerodynamic fineness against angle of attack.

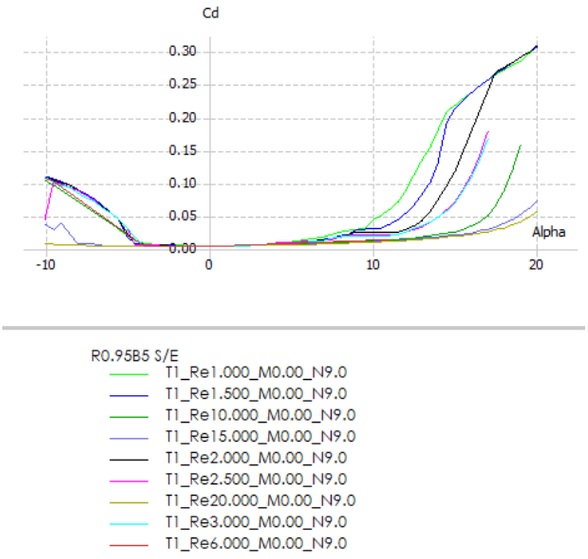

Figure 3.4 Qblade software results of the R0.9B5 profile coefficient of drag versus angle of attack.

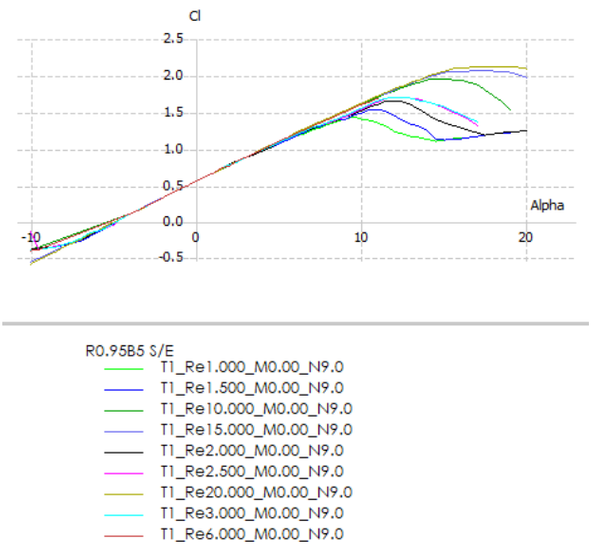

Figure 3.5 Results of the Qblade software of the R0.95B5 profile coefficient of lift versus angle of attack.

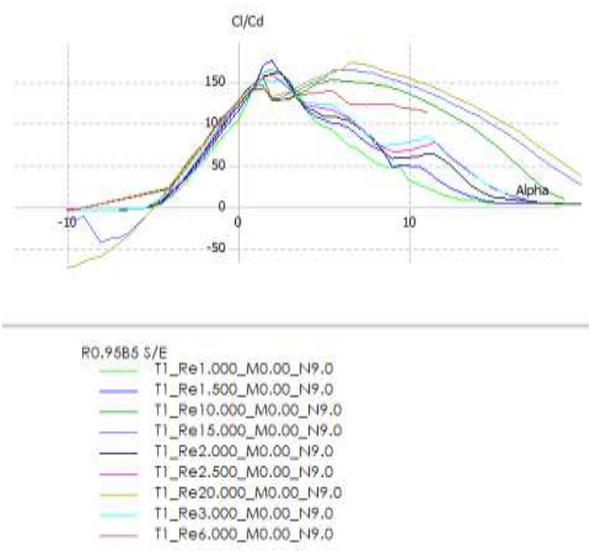

Figure 3.6 Results of the Qblade software of the profile R0.95B5 aerodynamic fineness against angle of attack.

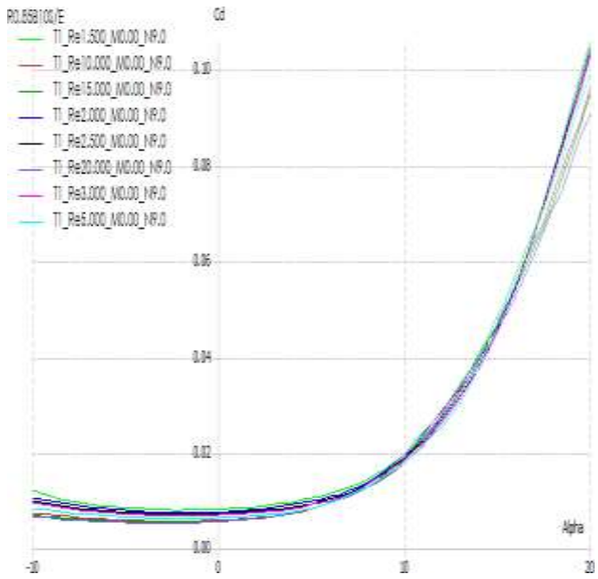

Figure 3.7 Qblade software results of profile R0.85B10 coefficient of drag versus angle of attack.

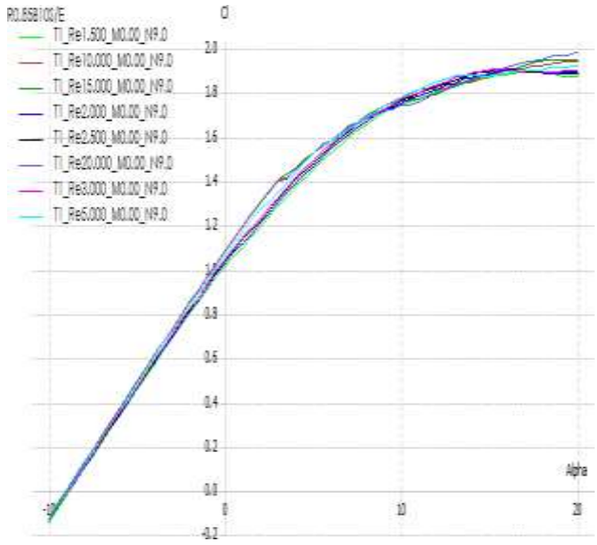

Figure 3.8 Qblade software results of the R0.85B10 profile coefficient of lift versus angle of attack.

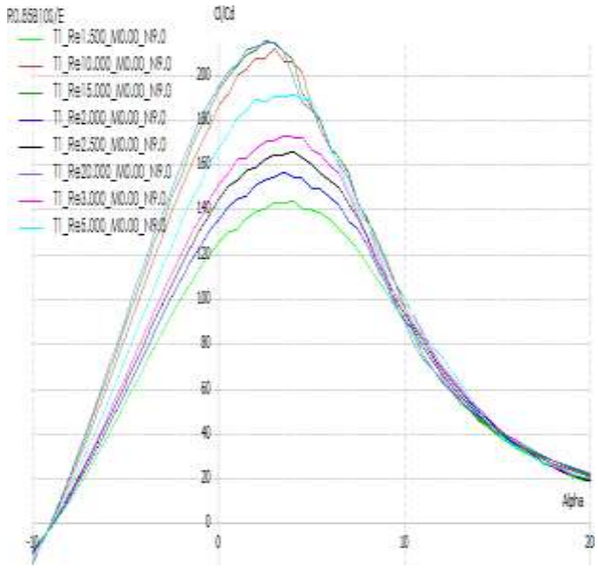

Figure 3.9 Results of the Qblade software of the profile R0.85B10 aerodynamic fineness against angle of attack.

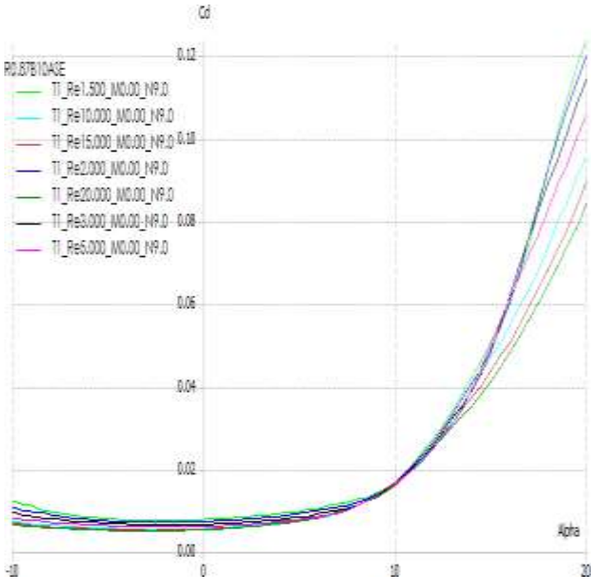

Figure 3.10 Results of the Qblade software of the profile R0.87B10 drag coefficient against the angle of attack.

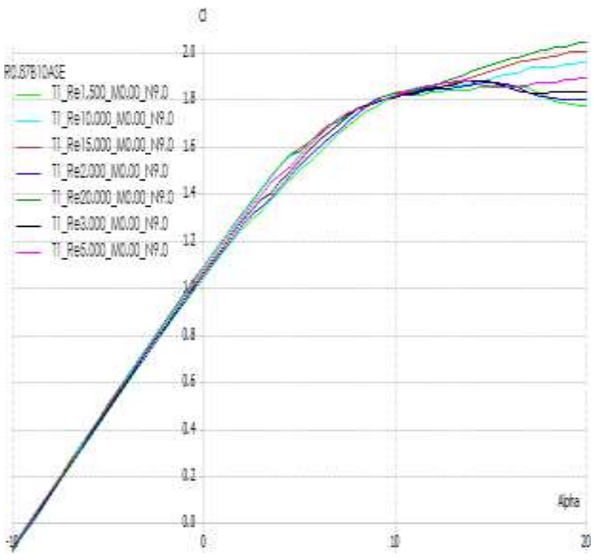

Figure 3.11 Results of the Qblade software of the profile R0.87B10 coefficient of lift against angle of attack

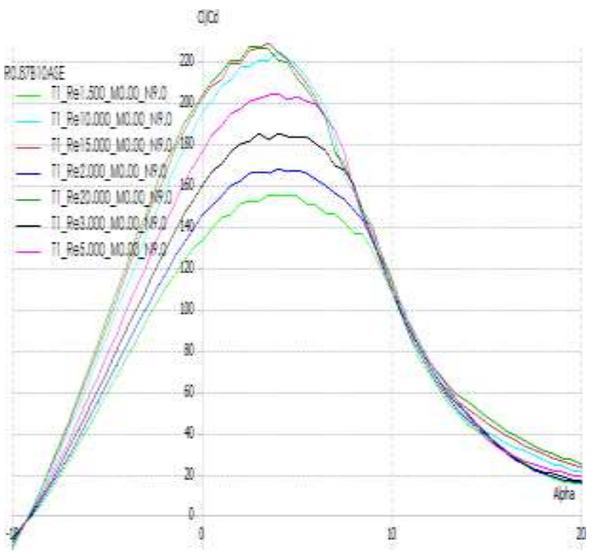

Figure 3.12 Results of the Qblade software of the profile R0.87B10 coefficient of lift against angle of attack

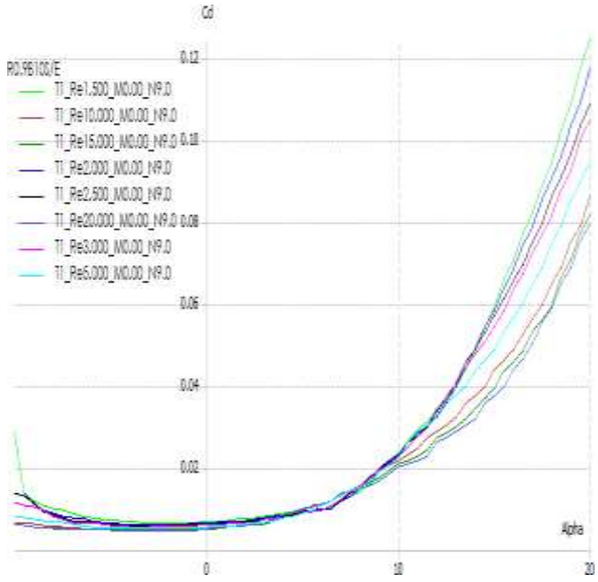

Figure 3.13 Results of the Qblade software of the profile R0.9B10 drag coefficient against the angle of attack.

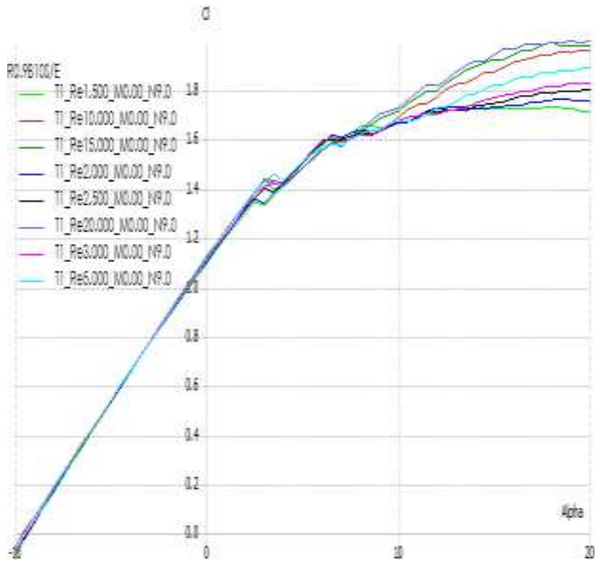

Figure 3.14 Results of the Qblade software of the profile R0.9B10 coefficient of lift versus angle of attack.

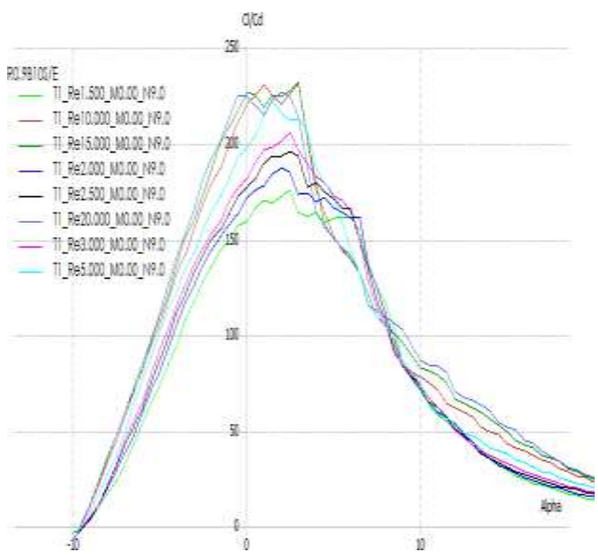

Figure 3.15 Results of the Qblade software of the profile R0.9B10 aerodynamic fineness against angle of attack.

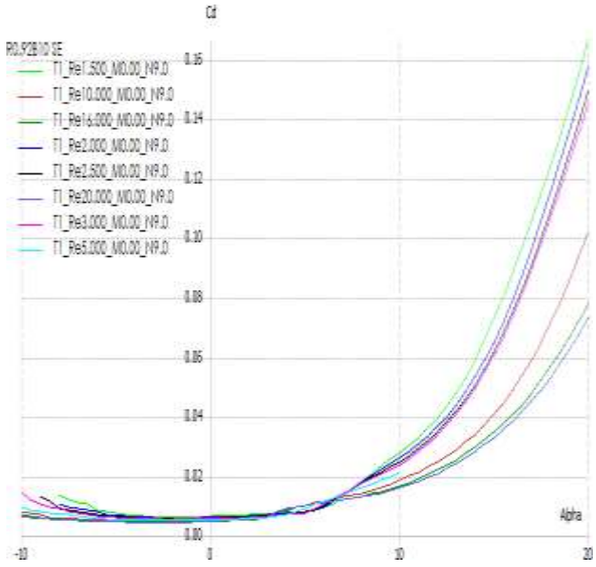

Figure 3.16 Qblade software results of profile R0.9B10 coefficient of drag versus angle of attack

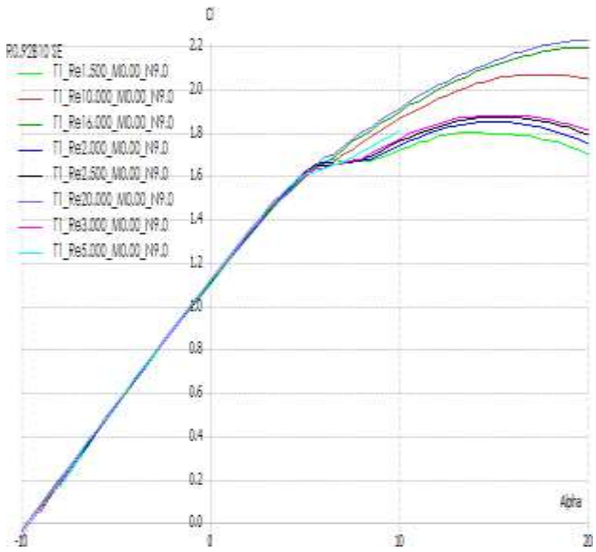

Figure 3.17 Results of the Qblade software of the profile R0.92B10 coefficient of lift against angle of attack

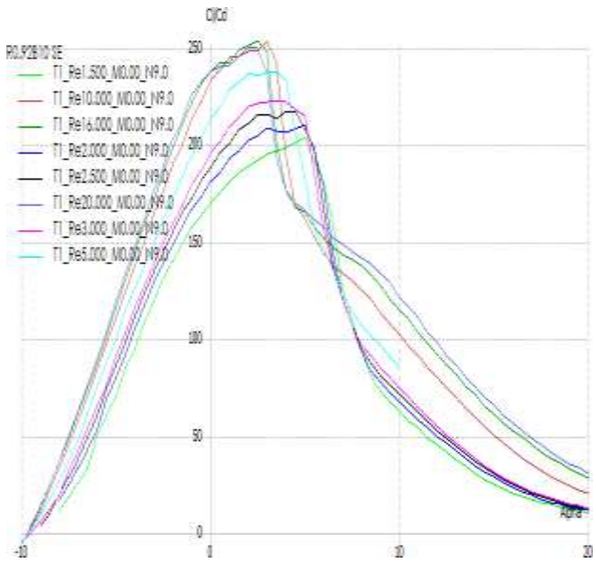

Figure 3.18 Results of the Qblade software of the profile R0.92B10 aerodynamic fineness against angle of attack.

4. Transition points of the wing profiles

The transition points are the coordinates defined in percentage of the chord where the laminar flow around the wing profile changes to a transitory or turbulent one due to the laminar separation bubble, these points are provided by the software, these coordinates being called "Upper trans "," Upper transition "refers to the transition in the upper surface, while the term" Lower trans "refers to" Lower transition ", which indicates the transition point of the flow in the intrados.

Profile R0.9B5A0		
Attack angle 0 °		
Reynolds	**Upper transition**	**Lower transition**
1.5x10^6	62.60%	30.30%
2x10^6	60.00%	27.50%
2.5x10^6	56.60%	25.80%
3x10^6	53.50%	24.10%
5x10^6	46.80%	20.70%
11x10^6	37.70%	16.30%
15x10^6	36.00%	14.20%
20x10^6	32.30%	14.00%

Table 4.1 Transition points of profile R0.9B5A0

Table 4.1 indicates that the profile achieves, for an angle of attack equal to zero, to generate under small Reynolds numbers, for example for a Reynolds number of 3 million, the laminar flow reaches up to 53.3% of its chord in the extrados , while in the intrados the laminar flow begins to form up to 24.1% of the chord of the wing profile, in addition, its performance for high Reynolds numbers, for example 11 million, is acceptable since the profile is capable to maintain a laminar flow up to 37.7% of its chord while the laminar flow in the ceiling appears up to 16.3% of it.

Table 4.2 indicates that the profile achieves, for an angle of attack equal to 2.5°, to generate under small Reynolds numbers, equal to 3 million, a laminar flow of up to 37.6% of its chord in the extrados, while in the intrados laminar flow begins to form up to 44.7% of the chord of the wing profile, in addition, its performance at high Reynolds numbers, of 11 million, allows a laminar flow to be obtained on most soffits but not on the extrados, since the profile is capable of maintaining laminar flow up to 28% of its chord while laminar flow in the intrados appears up to 29.5% of it.

ISSN 2523-6776

Table 4.3 indicates that the profile achieves, for an angle of attack equal to 5 °, to generate under small Reynolds numbers, than 3 million, a laminar flow up to 27.7% of its chord on the extrados, while in the intrados laminar flow begins to form up to 61% of the chord of the wing profile, in addition, its performance for high Reynolds numbers, than 11 million, allows a laminar flow to be obtained over most of the intrados but not over the extrados , since the profile is capable of maintaining laminar flow up to 17.1% of its chord while laminar flow in the intrados appears up to 48.6% of it.

Profile R0.9B5A2.5		
Angle of attack 2.5 °		
Reynolds	**Upper transition**	**Lower transition**
1.5x10^6	44.70%	53.80%
2x10^6	41.20%	50.20%
2.5x10^6	39.80%	47.30%
3x10^6	37.60%	44.70%
5x10^6	33.70%	38.90%
11x10^6	28.00%	29.50%
15x10^6	24.70%	26.30%
20x10^6	23.70%	24.10%

Table 4.2 Transition points of profile R0.9B5A2.5

Profile R0.9B5A5		
Angle of attack 5 °		
Reynolds	**Upper transition**	**Lower transition**
1.5x10^6	31.70%	67.70%
2x10^6	29.80%	65.10%
2.5x10^6	28.10%	63.30%
3x10^6	27.70%	61.00%
5x10^6	23.90%	58.00%
11x10^6	17.10%	48.60%
15x10^6	14.10%	44.60%
20x10^6	11.70%	40.60%

Table 4.3 Transition points of profile R0.9B5A5

Table 4.4 indicates that the profile achieves, for an angle of attack equal to 7.5 °, to generate under small Reynolds numbers, than 3 million, a laminar flow up to 11.4% of its chord on the extrados, while in the intrados the laminar flow is never formed, in addition, its performance for high Reynolds numbers, than 11 million, allows to obtain a laminar flow over most of the intrados but not over the extrados, since the profile is capable of maintaining a flow laminar up to 5% of its chord while laminar flow in the soffit appears up to 60.9% of it.

The tables of the transition points are located in the annexes, the first annex contains the tables of the transition points of the R0.95B5 profile, the second annex the tables of the R0.85B10 profile, the third annex the tables of the R0 profile. 87B10, the fourth appendix the tables of the profile R0.9B10 and the fifth the tables of the profile R0.92B10.

Profile R0.9B5A7.5		
ngle of attack 7.5 °		
Reynolds	**Upper transition**	**Lower transition**
1.5x10^6	20.30%	100.00%
2x10^6	16.50%	100.00%
2.5x10^6	13.50%	100.00%
3x10^6	11.40%	100.00%
5x10^6	7.80%	69.60%
11x10^6	5.00%	60.90%
15x10^6	3.60%	60.10%
20x10^6	2.50%	56.40%

Table 4.4 Transition points of profile R0.9B5A7.5

Conclusions

1. It was found that the curvature in the contour of the profile causes an increase in the lift coefficient, a fact that is corroborated by the circulation equation, and in addition, the relationship between the lift coefficient and the drag coefficient is wider, consequently A thin profile with the appropriate curvature generates a greater aerodynamic fineness compared to a thicker one, in addition, in theory the thin profile can develop a greater lift coefficient than a thick thick one, this can be observed if the performances performed by the profiles R0.92B10 and R0.87B10.

2. The Joukowsky transformation allows to obtain aerodynamic profiles with satisfactory performance values, but due to the uniqueness in the "-b" coordinate, the transformation generates a very sharp trailing edge.

3. Analysis by Theodorsen method is not effective for thin and some medium airfoils, check Table 1 from the annex 6.

4. Thicker profiles tend to perform better at high angles of attack compared to thinner profiles.

ISSN 2523-6776

5. The thicker profiles better preserve the boundary layer on the surface by increasing the angle of attack compared to the thin profiles, see tables of the transition points of profile R0.85B10.

6. Thin wing profiles at high angles of attack generate very high drag coefficients and turbulent flows over the surface, see profile tables R0.95B5, R0.9B5, R0.92B10 and R0.9B10.

7. It was found that, in theory, as the Reynolds number increases, the flow on the upper surface becomes turbulent, while on the lower surface the flow becomes laminar.

Acknowledgements

To the Universidad Michoacana de San Nicolás de Hidalgo for providing the tools for research.

To FIM, Facultad de Ingeniería Mecánica
.
To the RETANA-VEGA, Dzoara, Estefanía. BsC, for her support in this work.

Annexes

Annex 1

Table 4.5 indicates that the R0.95B5 profile achieves, for an angle of attack equal to zero, to generate under small Reynolds numbers, than 3 million, a laminar flow up to 69% of its chord on the extrados, while in the intrados the laminar flow begins to form up to 27.4% of the chord of the wing profile, in addition, its performance for high Reynolds numbers, than 11 million, is satisfactory since the profile is capable of maintaining a laminar flow up to 49.1% of its chord while laminar flow in the soffit appears up to 13.9% of it.

Profile R0.95B5A0		
Attack angle 0 °		
Reynolds	**Upper transition**	**Lower transition**
1.5x10^6	75.80%	34.10%
2x10^6	73.50%	31.10%
2.5x10^6	71.20%	29.10%
3x10^6	69.00%	27.40%
5x10^6	60.40%	20.70%
11x10^6	49.10%	13.90%
15x10^6	44.00%	12.00%
20x10^6	38.80%	10.30%

Table 4.5 Transition points of profile R0.95B5A0

Table 4.6 indicates that the profile achieves, for an angle of attack equal to 3 °, to generate under small Reynolds numbers, of 3 million, a laminar flow of up to 19.8% of its chord on the extrados, although it is important Note that at this angle of attack, the boundary layer is dramatically affected in a negative way as the Reynolds number increases in the analyzes, in the intrados no laminar flow is generated at any point of the chord of the wing profile, in addition , its performance for high Reynolds numbers, higher than 11 million, allows a laminar flow to be obtained over most of the intrados but not over the extrados, since the profile is capable of maintaining a laminar flow up to 3.7% of its chord while laminar flow in the soffit appears up to 41.2% of it.

Profile R0.95B5A3		
Angle of attack 3 °		
Reynolds	**Upper transition**	**Lower transition**
1.5x10^6	40.90%	100.00%
2x10^6	31.60%	100.00%
2.5x10^6	24.40%	100.00%
3x10^6	19.80%	100.00%
5x10^6	10.80%	69.60%
11x10^6	3.70%	41.20%
15x10^6	3.20%	34.40%
20x10^6	1.50%	27.70%

Table 4.6 Transition points of profile R0.95B5A3

Profile R0.95B5A7		
Angle of attack 7 °		
Reynolds	**Upper transition**	**Lower transition**
1.5x10^6	0.50%	100.00%
2x10^6	0.40%	100.00%
2.5x10^6	0.30%	100.00%
3x10^6	0.30%	100.00%
5x10^6	0.30%	100.00%
11x10^6	0.20%	100.00%
15x10^6	0.20%	100.00%
20x10^6	0.20%	100.00%

Table 4.7 Transition points of profile R0.95B5A7

Table 4.7 indicates that the profile R0.95B5A7 achieves, for an angle of attack equal to 7 °, to generate under small Reynolds numbers, than 3 million, a laminar flow up to 0.3% of its chord on the extrados, while in the intrados does not generate laminar flow, in addition, its performance for high Reynolds numbers, greater than 11 million, the profile maintains its laminar flow up to 0.2% of its chord on the extrados, on the other hand, in the intrados, all the flow on the surface it is turbulent.

Annex 2

Table 4.8 indicates that the R0.85B10 profile achieves, for an angle of attack equal to zero, to generate under small Reynolds numbers, than 3 million, a laminar flow of 53.9% of its chord on the extrados, while in the intrados the laminar flow begins to form up to 17.8% of the chord of the wing profile, in addition, its performance for high Reynolds numbers, than 10 million, is acceptable since the profile is capable of maintaining a laminar flow up to the 48.2% of its chord while laminar flow in the soffit appears up to 14.3% of it.

Profile R0.85B10A0		
Attack angle 0 °		
Reynolds	**Upper transition**	**Lower transition**
1.5x10^6	56.80%	19.80%
2x10^6	55.50%	18.90%
2.5x10^6	54.60%	18.40%
3x10^6	53.90%	17.80%
5x10^6	51.40%	16.50%
10x10^6	48.20%	14.30%
15x10^6	45.70%	13.00%
20x10^6	43.40%	12.30%

Table 4.8 Transition points of profile R0.85B10A0

Profile R0.85B10A3		
Angle of attack 3 °		
Reynolds	**Upper transition**	**Lower transition**
1.5x10^6	51.90%	27.80%
2x10^6	50.60%	26.50%
2.5x10^6	49.60%	26.10%
3x10^6	48.50%	25.70%
5x10^6	46.10%	23.70%
10x10^6	41.70%	22.30%
15x10^6	37.70%	21.10%
20x10^6	35.20%	19.80%

Table 4.9 Transition points of profile R0.85B10A3

Table 4.9 indicates that the profile achieves, for an angle of attack equal to 3 °, to generate under small Reynolds numbers, than 3 million, a laminar flow of 48.5% of its chord on the extrados, while on the intrados laminar flow begins to form up to 25.7% of the chord of the wing profile, in addition, its performance for high Reynolds numbers, than 10 million, is acceptable since the profile is capable of maintaining a laminar flow up to 41.7% of its chord while laminar flow in the soffit appears up to 22.3% of it.

Table 4.10 indicates that the profile achieves, for an angle of attack equal to 7 °, to generate under small Reynolds numbers, than 3 million, a laminar flow of 39.2% of its chord on the extrados, while in the intrados laminar flow begins to form up to 37.7% of the chord of the wing profile, in addition, its performance for high Reynolds numbers, than 10 million, is acceptable since the profile is capable of maintaining a laminar flow up to 26.4% of its chord while the laminar flow in the intrados appears up to 31.4% of it.

Profile R0.85B10A7		
Angle of attack 7 °		
Reynolds	**Upper transition**	**Lower transition**
1.5x10^6	44.00%	42.60%
2x10^6	42.10%	40.50%
2.5x10^6	40.70%	39.20%
3x10^6	39.20%	37.70%
5x10^6	33.00%	34.60%
10x10^6	26.40%	31.40%
15x10^6	22.20%	28.90%
20x10^6	19.30%	28.20%

Table 4.10 Transition points of profile R0.85B10A7

Table 4.11 indicates that the profile achieves, for an angle of attack equal to 14 °, to generate under small Reynolds numbers, than 3 million, a laminar flow up to 17.7% of its chord on the extrados, while in the intrados the flow is never laminar, in addition, for high Reynolds numbers, than 10 million, the profile is capable of maintaining a laminar flow up to 5.3% of its chord while the laminar flow in intrados is never generated.

Profile R0.85B10A14		
Angle of attack 14 °		
Reynolds	**Upper transition**	**Lower transition**
1.5x10^6	22.30%	100.00%
2x10^6	20.50%	100.00%
2.5x10^6	19.00%	100.00%
3x10^6	17.70%	100.00%
5x10^6	12.50%	100.00%
10x10^6	5.30%	100.00%
15x10^6	2.90%	60.30%
20x10^6	1.70%	53.90%

Table 4.11 Transition points of profile R0.85B10A14

ISSN 2523-6776

Table 4.12 indicates that the profile achieves, for an angle of attack equal to 20 °, to generate under small Reynolds numbers, than 3 million, a laminar flow up to 5.4% of its chord on the extrados, while in the intrados the flow is never laminar, in addition, for high Reynolds numbers, than 10 million, the profile is capable of maintaining a laminar flow up to 1.3% of its chord while the laminar flow in intrados is never generated again.

Profile R0.85B10A20		
Angle of attack 20°		
Reynolds	**Upper transition**	**Lower transition**
1.5x10^6	9.00%	100.00%
2x10^6	7.40%	100.00%
2.5x10^6	6.10%	100.00%
3x10^6	5.40%	100.00%
5x10^6	3.50%	100.00%
10x10^6	1.30%	100.00%
15x10^6	0.50%	100.00%
20x10^6	0.40%	100.00%

Table 4.12 Transition points of profile R0.85B10A20

Annex 3

Profile R0.87B10A0		
Attack angle 0°		
Reynolds	**Upper transition**	**Lower transition**
1.5x10^6	57.20%	19.80%
2x10^6	56.30%	19.10%
2.5x10^6	55.10%	18.50%
3x10^6	54.40%	17.80%
5x10^6	52.00%	16.10%
10x10^6	48.90%	13.90%
15x10^6	46.20%	13.00%
20x10^6	43.70%	12.00%

Table 4.13 Transition points of profile R0.87B10A0

Table 4.13 indicates that the profile achieves, for an angle of attack equal to zero, to generate under small Reynolds numbers, than 3 million, a laminar flow up to 54.4% of its chord on the extrados, while on the intrados laminar flow begins to form up to 17.8% of the chord of the wing profile, in addition, its performance for high Reynolds numbers, than 10 million, is satisfactory since the profile is capable of maintaining a laminar flow up to 48.9% of its chord while the laminar flow in the soffit appears up to 13% of it.

Table 4.14 indicates that the profile achieves, for an angle of attack equal to 3 °, to generate under small Reynolds numbers, than 3 million, a laminar flow up to 48.7% of its chord on the extrados, while in the intrados the laminar flow begins to form up to 25.3% of the chord of the wing profile, in addition, its performance for high Reynolds numbers, than 10 million, allows to obtain a laminar flow, since the profile is capable of maintaining a flow laminar up to 41.5% of its chord while laminar flow in the soffit appears up to 21.7% of it.

Profile R0.87B10A3		
Angle of attack 3 °		
Reynolds	**Upper transition**	**Lower transition**
1.5x10^6	52.00%	27.20%
2x10^6	50.90%	25.90%
2.5x10^6	49.60%	25.60%
3x10^6	48.70%	25.30%
5x10^6	45.90%	23.60%
10x10^6	41.50%	21.70%
15x10^6	38.60%	21.10%
20x10^6	35.80%	19.90%

Table 4.14 Transition points of profile R0.87B10A3

Table 4.14 indicates that the profile achieves, for an angle of attack equal to 3 °, to generate under small Reynolds numbers, than 3 million, a laminar flow up to 48.7% of its chord on the extrados, while in the intrados the laminar flow begins to form up to 25.3% of the chord of the wing profile, in addition, its performance for high Reynolds numbers, than 10 million, allows to obtain a laminar flow, since the profile is capable of maintaining a flow laminar up to 41.5% of its chord while laminar flow in the soffit appears up to 21.7% of it.

Profile R0.87B10A5		
Angle of attack 5 °		
Reynolds	**Upper transition**	**Lower transition**
1.5x10^6	48.30%	33.60%
2x10^6	46.80%	32.50%
2.5x10^6	45.60%	31.20%
3x10^6	44.60%	30.70%
5x10^6	42.00%	28.40%
10x10^6	36.90%	25.90%
15x10^6	30.30%	25.80%
20x10^6	28.80%	23.60%

Table 4.15 Transition points of profile R0.87B10A5

ISSN 2523-6776

Table 4.15 indicates that the profile achieves, for an angle of attack equal to 5 °, to generate under small Reynolds numbers, than 3 million, a laminar flow up to 44.6% of its chord on the extrados, while in the intrados the laminar flow begins to form up to 30.7% of the chord of the wing profile, in addition, its performance for high Reynolds numbers, than 10 million, allows to obtain a laminar flow, since the profile is capable of maintaining a flow laminar up to 36.90% of its chord while laminar flow in the soffit appears up to 25.8% of it.

Profile R0.87B10A7.5		
Angle of attack 7.5 °		
Reynolds	**Upper transition**	**Lower transition**
1.5x10^6	43.50%	54.70%
2x10^6	41.80%	49.40%
2.5x10^6	40.10%	46.10%
3x10^6	39.30%	44.40%
5x10^6	34.60%	39.20%
10x10^6	24.40%	33.40%
15x10^6	19.00%	32.70%
20x10^6	18.60%	29.20%

Table 4.16 Transition points of profile R0.87B10A7.5

Table 4.16 indicates that the profile achieves, for an angle of attack equal to 7.5 °, to generate under small Reynolds numbers, than 3 million, a laminar flow up to 39.3% of its chord on the extrados, while in the intrados the laminar flow begins to form up to 44.4% of the chord of the wing profile, in addition, its performance for high Reynolds numbers, than 10 million, allows to obtain a laminar flow up to 24.4% of its chord while the flow laminar on the intrados appears up to 33.4% of it.

Profile R0.87B10A10		
Angle of attack 10 °		
Reynolds	**Upper transition**	**Lower transition**
1.5x10^6	34.80%	100.00%
2x10^6	31.20%	100.00%
2.5x10^6	28.20%	100.00%
3x10^6	25.70%	100.00%
5x10^6	20.00%	68.30%
10x10^6	14.70%	46.00%
15x10^6	11.20%	40.80%
20x10^6	8.20%	37.70%

Table 4.17 Transition points of profile R0.87B10A10

Table 4.17 indicates that the profile achieves, for an angle of attack equal to 10 °, to generate under small Reynolds numbers, less than 3 million, a laminar flow up to 25.7% of its chord on the extrados, while in the intrados laminar flow does not appear for these conditions, its performance for high Reynolds numbers, greater than 10 million, the profile is capable of maintaining laminar flow up to 14.7% of its chord while laminar flow in the intrados appears up to 46% of it.

Annex 4

Profile R0.9B10A0		
Attack angle 0 °		
Reynolds	**Upper transition**	**Lower transition**
1.5x10^6	61.50%	18.50%
2x10^6	60.40%	16.60%
2.5x10^6	59.00%	16.10%
3x10^6	57.20%	15.30%
5x10^6	55.10%	13.40%
10x10^6	52.00%	10.70%
15x10^6	48.90%	9.20%
20x10^6	44.90%	8.60%

Table 4.18 Transition points of profile R0.9B10A0

Table 4.18 indicates that the profile achieves, for an angle of attack equal to zero, to generate under small Reynolds numbers, than 3 million, a laminar flow up to 57.7% of its chord on the extrados, while in the intrados laminar flow begins to form up to 15.3% of the chord of the wing profile, in addition, its performance for high Reynolds numbers, than 10 million, is very satisfactory since the profile is capable of maintaining a laminar flow up to 52 % of its chord while laminar flow in the intrados appears up to 10.7% of it.

Profile R0.9B10A3		
Angle of attack 3 °		
Reynolds	**Upper transition**	**Lower transition**
1.5x10^6	54.90%	31.80%
2x10^6	53.00%	30.90%
2.5x10^6	51.40%	30.90%
3x10^6	48.90%	29.80%
5x10^6	44.80%	28.10%
10x10^6	40.50%	25.20%
15x10^6	36.50%	22.40%
20x10^6	32.70%	19.40%

Table 4.19 Transition points of profile R0.9B10A3

ISSN 2523-6776

Table 4.19 indicates that the profile achieves, for an angle of attack equal to 3 °, to generate under small Reynolds numbers, than 3 million, a laminar flow up to 48.9% of its chord on the extrados, while in the intrados the laminar flow begins to form up to 29.8% of the chord of the wing profile, in addition, its performance for high Reynolds numbers, than 10 million, is satisfactory since the profile is capable of maintaining a laminar flow up to 40.5 % of its chord while laminar flow in the intrados appears up to 25.2% of it.

Profile R0.9B10A6		
Attack angle 6 °		
Reynolds	**Upper transition**	**Lower transition**
1.5x10^6	44.70%	100.00%
2x10^6	41.20%	67.60%
2.5x10^6	39.70%	56.80%
3x10^6	36.70%	47.50%
5x10^6	24.00%	37.70%
10x10^6	13.40%	32.00%
15x10^6	8.50%	30.80%
20x10^6	4.60%	29.00%

Table 4.20 Transition points of profile R0.9B10A6

Table 4.20 indicates that the profile achieves, for an angle of attack equal to 6 °, to generate under small Reynolds numbers, than 3 million, a laminar flow up to 36.7% of its chord on the extrados, while in the intrados the laminar flow begins to form up to 47.5% of the chord of the wing profile, in addition, its performance for high Reynolds numbers, than 10 million, the profile is capable of maintaining a laminar flow up to 13.4% of its chord while laminar flow in the intrados appears up to 32% of it.

Profile R0.9B10A8		
Angle of attack 8 °		
Reynolds	**Upper transition**	**Lower transition**
1.5x10^6	33.50%	100.00%
2x10^6	26.60%	100.00%
2.5x10^6	21.20%	100.00%
3x10^6	17.70%	100.00%
5x10^6	11.30%	100.00%
10x10^6	4.60%	42.70%
15x10^6	1.60%	37.70%
20x10^6	0.70%	35.10%

Table 4.21 Transition points of profile R0.9B10A8

Table 4.21 indicates that the profile achieves, for an angle of attack equal to 8 °, to generate under small Reynolds numbers, than 3 million, a laminar flow up to 17.7% of its chord on the extrados, while in the intrados the flow is never generated, in addition, its performance for high Reynolds numbers, than 10 million, the profile is capable of maintaining a laminar flow up to 4.6% of its chord while the laminar flow in the intrados appears up to 42.7 % Of the same.

Annex 5

Table 4.22 indicates that the profile achieves, for an angle of attack equal to zero, to generate under small Reynolds numbers, than 3 million, a laminar flow up to 61.8% of its chord on the extrados, while on the intrados laminar flow begins to form up to 14% of the chord of the wing profile, in addition, its performance for high Reynolds numbers, greater 10 million, is satisfactory since the profile is capable of maintaining a laminar flow up to 55% of its chord while laminar flow in the soffit appears up to 10% of it.

Profile R0.92B10A0		
Attack angle 0 °		
Reynolds	**Upper transition**	**Lower transition**
1.5x10^6	65.80%	16.60%
2x10^6	64.10%	15.30%
2.5x10^6	62.50%	14.70%
3x10^6	61.80%	14.00%
5x10^6	59.10%	12.40%
10x10^6	55.00%	10.00%
16x10^6	51.10%	9.10%
20x10^6	48.40%	8.30%

Table 4.22 Transition points of profile R0.92B10A0

Profile R0.92B10A3		
Angle of attack 3 °		
Reynolds	**Upper transition**	**Lower transition**
1.5x10^6	58.60%	39.50%
2x10^6	57.00%	36.70%
2.5x10^6	55.20%	34.80%
3x10^6	53.80%	33.20%
5x10^6	50.00%	29.80%
10x10^6	45.00%	24.90%
16x10^6	38.50%	21.80%
20x10^6	33.60%	21.00%

Table 4.23 Transition points of profile R0.92B10A3

ISSN 2523-6776

Table 4.23 indicates that the profile achieves, for an angle of attack equal to 3 °, to generate under small Reynolds numbers, than 3 million, a laminar flow up to 53.8% of its chord on the extrados, while in the intrados the laminar flow begins to form up to 33.2% of the chord of the wing profile, in addition, its performance for high Reynolds numbers, than 10 million, is satisfactory since the profile is capable of maintaining a laminar flow up to 45 % of its chord while laminar flow in the intrados appears up to 24.9% of it.

Table 4.24 indicates that the profile achieves, for an angle of attack equal to 5 °, to generate under small Reynolds numbers, than 3 million, a laminar flow up to 42.6% of its chord on the extrados, while in the intrados the laminar flow begins to form up to 93% of the chord of the wing profile, in addition, its performance for high Reynolds numbers, than 10 million, the profile is capable of maintaining a laminar flow up to 12.7% of its chord while the laminar flow in the intrados appears up to 35.5% of it.

Profile R0.92B10A5		
Angle of attack 5 °		
Reynolds	**Upper transition**	**Lower transition**
1.5x10^6	51.80%	100.00%
2x10^6	48.00%	100.00%
2.5x10^6	45.2%	100.00%
3x10^6	42.60%	93.00%
5x10^6	29.80%	45.80%
10x10^6	12.70%	35.50%
16x10^6	7.50%	31.40%
20x10^6	5.40%	30.20%

Table 4.24 Transition points of profile R0.92B10A5

Annex 6

Comparison of the results of the lift coefficients, at an angle identical to zero					
0	**1**	**2**	**3**	**4**	**5**
Profile name	Cl of the equation (3.6.6.1)	Cl of the analysis in the XFLR5 softwar, in Qblade	Cl of Theodorsen's method	Percentage difference of 1 with respect to 2	Percentage difference of 3 with respect to 2
R0.9B5A0	0.54	0.56	0.73	3.57%	-30.35%
R0.95B5A0	0.54	0.54	0.4	0%	25.9%
R0.85B10A	1.09	1.05	1.088	-3.8%	-3.61%
R0.87B10A0	1.09	1.06	1.082	-2.83	-2.075%
R0.9B10A0	1.09	1.1	0.88	0.9%	20%
R0.92B10A0	1.09	1.11	0.68	1.8%	38.73%

Table 1 Comparison of the results between the three methodologies

References

Carmona, Anibal Isidoro. *Aerodinámica y actuaciones del avion.* Madrid : Paraninfo, 2000.

Chattot, J.J y Hafez, M.M. *Theoretical and Applied Aerodynamics.* New York : Springer, 2015.

Galindo, Diego Rodrigo Flores. *Diseño de perfiles aerodinámicos.* Ciudad de México : s.n., 2006.

Gómez, Gabriel Adrián Romero. *Diseño de perfiles alares.* Morelia : s.n., 2021.

H. Abbott, Ira y Von Doenhoff, Albert E. *Theory of wing section.* New York : McGraw-Hill, 1959.

John D. Anderson, Jr. *Fundamentals of Aerodynamics.* Maryland : McGraw-Hill, 1991.

Katz, Joseph y Plotkin, Allen. *Low-Speed Aerodynamics.* New York : Cambrige University press, 2010.

McCormick, Barnes W. *Aerodinamics, aeronautics, and flight mechanics.* New York : Pennsylvania State University, 1979.

Tejada, Lina Alejandra. *Estudio de algunos perfiles aerodinámicos.* Bogotá : s.n., 2020.

White, Frank M. *Mecánica de fluidos.* s.l. : McGraw-Hill, 2010.